ELSEVIER

Journal of Power Sources 110 (2002) 406–411

JOURNAL OF POWER SOURCES

www.elsevier.com/locate/jpowsour

Lithium reactions with intermetallic-compound electrodes

R. Benedek*, M.M. Thackeray

Argonne National Laboratory, Argonne, IL 60439, USA

Abstract

Intermetallic compounds are under investigation as possible anode materials in lithium batteries. The compounds on which the Argonne National Laboratory group has primarily focused were selected on the basis of structural compatibility between host and product (lithiated) phases. In this presentation, we discuss the additional insights into the behavior of intermetallic-compound anodes that are available from materials modeling.

Keywords: Intermetallic compound; Solid state reaction; Electrochemical potential; Insertion kinetics; First principles theory

1. Introduction

The presentation by Thackeray at this meeting highlighted measurements by the Argonne National Laboratory group on three intermetallic compounds, Cu_6Sn_5 [1], InSb [2] and Cu_2Sb [3]. The selection of these compounds was motivated primarily by the *structural compatibility* of the original compound with the product lithiated phase. Thus, the sublattice of the more active component of the intermetallic compound (Sn or Sb in the cited compounds) either remains invariant or suffers at most a moderate distortion in the product phase. The concept of structural compatibility has led to the identification of a promising class of materials, with structures related to zinc blende, that have the potential for superior electrochemical performance. In this presentation, we discuss the additional insights into the behavior of intermetallic compounds as anode materials that can be developed by more detailed theory and modeling.

In principle, modeling can address a wide variety of issues related to metallic electrodes. The emphasis in our own work is on atomic structure and structural transformations. In addition to the atomic scale phenomena that we focus on, important processes occur at a wide range of length and time scales. This multi-scale aspect of the electrode kinetics makes their modeling particularly challenging. We will attempt to present a viewpoint that reflects a broad perspective, so that the reader may better understand what the fundamental obstacles are.

2. Structural compatibility

If we demand strict structural compatibility, i.e. that the sublattice of the more active element be invariant, and that in addition the sublattice type be cubic-close packed, then the number of eligible compounds is severely restricted. A search of compound tables [4] reveals that only two families of III–V compounds satisfy these criteria. The lattice constants of these compounds, the IIIB-antimonide and IIIA- and rare-earth bismuthides, are plotted in Fig. 1 versus the atomic number of the cation. It is reasonable to suppose that volume invariance as well as structural invariance is desirable, and therefore also plotted in Fig. 1 (right ordinate scale) as horizontal lines are the lattice constants of the lithiated product phases Li_3Sb and Li_3Bi. The two compounds InSb and LaBi have the smallest lattice constant mismatch, both less than about 2%.

InSb has been studied extensively by the Argonne group, and by others, but electrochemical behavior of LaBi has not yet been studied. From the standpoint of structural compatibility, InSb is the most favorable system. As Thackeray pointed out, however, the performance of Cu_2Sb is superior to InSb, structural compatibility notwithstanding. Although structural compatibility appears important, it is, of course, not the only factor that influences performance. Some of the others will be discussed in the following sections.

3. Compounds under investigation

Intermetallic compounds have been investigated by several workers. Among the recently studied systems are the antimonides Zn_4Sb_3 [5], InSb [2], SnSb [6,7], $TiSb_2$ [8],

* Corresponding author.
E-mail address: benedek@anl.gov (R. Benedek).

0378-7753/02/$ – see front matter
PII: S0378-7753(02)00204-5

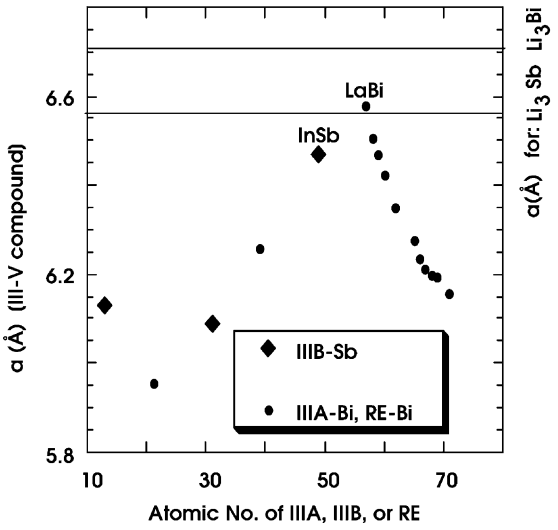

Fig. 1. Lattice constant data [4] for compounds of trivalent (group IIIA, IIIB and rare earth, RE) elements with Sb or Bi. The horizontal lines represent the lattice constants of Li_3Sb and Li_3Bi. The compounds InSb and LaBi give the smallest misfit (<2%) relative to the displacement product phase Li_3Sb or Li_3Bi.

VSb_2 [8], $CrSb_2$ [9], MnSb [10], $CoSb_3$ [11], Cu_2Sb [3], and $CoFe_3Sb_{12}$ [12], the stannides $MnSn_2$ [6], $Mn_{1.77}Sn$ [13], Mn_3Sn [13], Mn_3SnC [13,14], FeSn [15], $FeSn_2$ [8,16], $CoSn_2$ [8], Ni_3Sn_2 [17], Cu_6Sn_5 [1,18,19] and CaSn [20], and the silicides CrSi [21], NiSi [22,23], FeSi [23] and Mg_2Si [24,25]. There is also some work on chalcogenides [12], particularly in earlier literature (the listed citations given here are only representative, and not exhaustive). Most of these compounds do not satisfy the criteria of product–host structural compatibility, and perhaps as a consequence, the majority of them exhibit negligible reversibility (at room temperature) of the reactions with Li discussed later. Thus, typically, the less active component of the compound is extruded during the first discharge cycle, and the original compound is not restored upon cycling. In the later discussion, emphasis will be given to the compounds that exhibit substantial reversibility.

4. Solid state reactions of lithium

Three general types of reactions of Li with intermetallic compounds are possible. The reaction

$$x\mathrm{Li} + \mathrm{AB}_y \rightarrow \mathrm{Li}_x\mathrm{AB}_y \quad \text{(I)}$$

is referred to as a *reconstitution* or *addition* reaction. In general, the ternary product Li_xAB_y and the host AB_y have markedly different crystal structures. A second type of reaction,

$$x\mathrm{Li} + \mathrm{AB}_y \rightarrow \mathrm{Li}_x\mathrm{B}_y + \mathrm{A}, \quad \text{(II)}$$

in which one of the compound components is extruded, is referred to as a *displacement* reaction. A third type of reaction,

$$x\mathrm{Li} + \mathrm{AB}_y \rightarrow \mathrm{Li}_x\mathrm{A}_{1-z}\mathrm{B}_y + \mathrm{A}_z, \quad \text{(III)}$$

which we refer to as *mixed*, involves both addition and displacement, i.e. only a fraction z of component A is displaced, and a ternary product $Li_xA_{1-z}B_y$ is produced as well. We have adopted the convention in I–III that A is the less active and B is the more active element.

Displacement (or mixed) reactions do not occur in pure metals, but only in compounds. They have previously been studied primarily in oxides at elevated temperatures [26,27], and little is known about the systematics of lithium induced displacement reactions in intermetallic compounds at room temperature.

5. Reaction sequences

The reactions I–III represent the possible first reactions of a binary intermetallic compound. Typically, as the insertion proceeds, more than one reaction occurs. Thus, e.g. an addition or mixed reaction may be followed by a displacement reaction with respect to the ternary system, and this may be followed by further addition reactions (addition to either the host or the phase of the extruded component, A). We note that for some compounds, the relevant sequence of reactions may be ambiguous. In this case, the first principles calculations discussed below may be helpful in elucidating the true reaction sequence. The calculations indicate which sequences are feasible energetically, because each reaction in the sequence must have a negative enthalpy.

6. Electrochemical potentials

In this section we discuss the electrochemical potential for an intermetallic compound during the first discharge cycle, versus a lithium metal anode [28]. To simplify the discussion, only the first reaction will be considered, although we have pointed out that some compounds undergo a sequence of reactions. In Fig. 2, are plotted schematic potential curves as a function of lithium insertion. The curve labeled 'expt' is

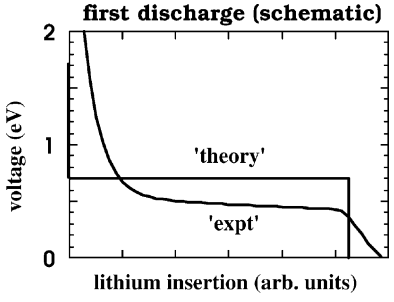

Fig. 2. Schematic voltage curve for the first discharge of an intermetallic-compound electrode versus lithium metal. The plateau region of the theoretical curve corresponds to a two-phase region, which starts when the solid solubility of Li in the original compound is exceeded. Since this solubility is essentially negligible, a vertical line is drawn at zero insertion. Experiment differs from this behavior in that an extended initial transient is often observed, which we attribute to extrinsic processes.

an idealization and does not represent actual data for a particular system. The steeply sloping part of the curve at small insertion represents an initial transient, which we attribute to extrinsic processes, such as reaction with the surface oxide. This transient is followed by a nearly flat plateau region that coincides with a reaction of type I, II or III. When the reaction is essentially complete, the electrochemical potential decreases sharply. If a sequence of reactions occurs, then additional plateau regions (not shown in the figure) may be observed.

The curve labeled 'theory' differs from experiment in that the extended initial transient is absent. A very narrow intrinsic transient is expected to occur as a result of configurational entropy, until the solubility of Li in the compound is reached. The equilibrium solid solubility of Li in most intermetallic compounds at room temperature is typically well below 0.01. The horizontal line in the theory curve corresponds to the flat part of the 'expt' curve, but is typically slightly above it as shown later.

7. Electrochemical potential prediction

In a cell that consists of a metallic Li anode and a metallic cathode, the electrochemical potential is defined as follows:

$$V = |\mu_{\mathrm{Li}}(\mathrm{product}) - \mu_{\mathrm{Li}}(\mathrm{Li})|, \tag{1}$$

where μ_{Li} is the chemical potential of Li either in the product phase or in metallic Li. Numerical calculations of the electrochemical potential for several metals and compounds were performed with the first principles local-density-functional theory VASP code [29,30], using the generalized gradient approximation (GGA) correction. The calculations correspond to zero temperature, however free energies at room temperature differ only slightly from those at lower temperatures. Calculated electrochemical potentials are plotted in Fig. 3 on the abscissa against experiment on the ordinate. The calculations systematically overestimatethe voltages, in part because the product phase is nucleated under stress in the matrix of the original compound or metal, whereas the calculations treat the product as stress free.

8. Lithium insertion kinetics

The reactions described earlier must be preceded by the diffusion of lithium into the metal or compound. Schematically, we can write the diffusion coefficient of Li interstitials as follows:

$$D \sim va^2 \exp\left(\frac{-E_{\mathrm{a}}}{k_{\mathrm{b}}T}\right) \sim \frac{l^2}{t}, \tag{2}$$

where v is an effective attempt frequency, a is the lattice constant, and k_{b} is Boltzmann's constant. For a fine-grained ball-milled specimen with characteristic length $l \sim 20$ m,

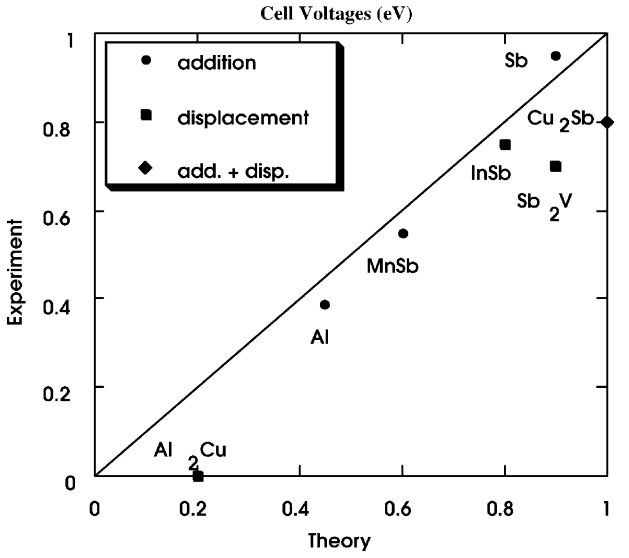

Fig. 3. Experimental vs. predicted cell voltages for Li-induced reactions with several intermetallic compounds and pure metals. Theoretical values were obtained with the VASP code [29,30], using the GGA. The experimental atomic structure, where known, was employed as the starting configuration, and lattice parameter and internal coordinates were optimized. In the case of pure Mn, an approximate antiferromagnetic structure for the 58-atom unit-cell was assumed. In the case of Al_2Cu, no electrochemical reaction was observed experimentally [8]. Calculations were performed for the ternary $LiAl_2Cu$, based on a hypothetical hexagonal structure. Similar voltages were predicted for addition and displacement reactions.

and choosing a time scale of 5 h, we find that diffusion will proceed at room temperature only if the activation energy E_{a} is less than about 0.5 eV. In relatively few metals have Li diffusion activation energies been measured. In one system of interest, InSb, it has been measured to be 0.3 eV, and bulk diffusion at room temperature therefore readily occurs. InSb is a relatively open structure, and therefore favorable for interstitial diffusion. Whether bulk diffusion at room temperature can occur readily in other compounds is not known. The fact that the reactions with a large number of compounds has been observed indicates that the activation energies either for bulk or short-circuit (grain-boundary, dislocation, etc.) diffusion is within the range of 0.5 eV or less.

9. Volume expansion

It is well known that one of the problems with metallic electrodes is the expansion that accompanies the reactions with Li. This expansion often leads to fracture, which may result in electrical isolation of part of the electrode. An example is Si, which can absorb up to 4.4 Li atoms,

$$4.4\,\mathrm{Li} + \mathrm{Si} \rightarrow \mathrm{Li}_{4.4}\mathrm{Si}, \tag{4}$$

and expands by a factor of 3.70 (volume of product divided by sum of volumes of reactants) in the process. Some other

reactions are as follows:

$$
\begin{aligned}
&3\,Li + InSb \rightarrow Li_3Sb + In && \text{volume expansion} = 1.42\\
&4\,Li + InSb \rightarrow Li_3Sb + LiIn && \text{volume expansion} = 1.62\\
&2\,Li + Cu_2Sb \rightarrow Li_2CuSb + Cu && \text{volume expansion} = 1.51\\
&3\,Li + Cu_2Sb \rightarrow Li_3Sb + 2\,Cu && \text{volume expansion} = 1.93\\
&10\,Li + Cu_6Sn_5 \rightarrow 5\,Li_2CuSn + Cu && \text{volume expansion} = 1.64\\
&22\,Li + Cu_6Sn_5 \rightarrow 5\,Li_{4.4}Sn + 6\,Cu && \text{volume expansion} = 2.84
\end{aligned}
\tag{5}
$$

These examples show that there is a wide variation in the fractional volume expansions of different metals (or semiconductors), when the reaction is carried to completion. On the other hand, the variation in the expansion per Li atom is much less. Fig. 4 shows the volume expansion per Li atom for Li-induced reactions with several intermetallic compounds and elemental materials. The systems are plotted on the abscissa scale in order of increasing volume expansion. The smallest volume expansion is that for LiC_6, intercalated graphite, and the largest is for body-centered cubic Li metal. Apart from InSb, whose volume expansion is similar to that of intercalated graphite, the other materials plotted show a variation of only about 15% in the volume expansion induced by reaction with Li. Not surprisingly, volume expansion alone is not a good predictor of a materials performance as a Li battery electrode. As discussed later, the performance of an electrode is determined by the complex interplay of several processes that accompany Li insertion.

The volume expansions presented earlier are based on the experimental data. Calculations based on first principles would give very similar results. First principles simulation can predict the volume expansion associated with interstitial Li dissolved in an intermetallic compound, which is difficult to measure experimentally. We present the results of such calculations here only for InSb and Cu_6Sn_5.

10. Kinetics of electrode evolution

In the preceding section, we noted that Li insertion into a metallic or compound electrode has two immediate consequences: (i) the equilibrium solubility limit of Li is exceeded at a low insertion level, and (ii) the Li induces volume expansion in the material. Both the supersaturation of Li and the induced volume expansion initiate the development of subsequent materials processes that influence intermetallic-compound electrode structural evolution and battery performance during insertion/extraction.

The Li supersaturation results in the nucleation and growth of Li-rich phases, in accordance with the reactions I, II or III. In the case of reactions II and III, this is accompanied by extrusion of the displaced component. The volume expansion induced by Li results in internal stress, plastic deformation, rupture and spallation. Thus, as the insertion of Li proceeds, atomic transport and chemical reactions occur, which are influenced by internal

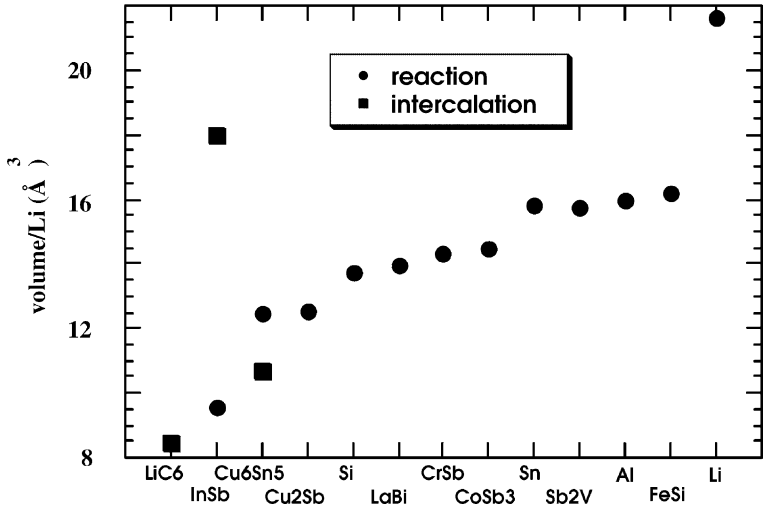

Fig. 4. Volume expansion per lithium atom for several intermetallic compounds and monatomic metals. The host systems are listed on the abscissa in order or increasing specific volume of reaction. The volume of reaction corresponds to the difference between the volume of the products and that of the original compound, per Li atom. The volume of intercalation corresponds to a Li atom in an interstitial site in a host matrix. The volumes of reaction were calculated based on experimental data, and the volumes of reaction for InSb and Cu_6Sn_5 were obtained from first principles calculations.

stresses, defect production and mechanical failure. These various processes are all coupled, and cannot be treated independently. The relevant length and time scales for the different processes range from the microscopic (e.g. for atomic diffusion) to the macroscopic (e.g. for fracture and spallation).

To model electrode performance, in principle, would require the development of a set of kinetic equations, which ideally would incorporate all of the relevant physical (chemical, atomic-transport and mechanical) processes. The solution to these spatio-temporal equations for suitably chosen boundary conditions (such as external current and geometry) would give information about the evolution of the electrode during battery operation. The voltage profile as a function of time and the capacity would be determined, as well as information about evolution of structure, phase distribution, and composition. Discharge and charge cycles would be treated by simulating, in turn, external currents in opposite directions. Capacity retention could be explored by examining the behavior upon repeated cycling.

Unfortunately, the battery-operation phenomena that we wish to describe go beyond the current state of the art of kinetic modeling. The most significant technical obstacles to modeling the kinetics of the intermetallic electrodes are (i) the multiple length and time scales involved, mentioned earlier, and (ii) the inhomogeneity of the atomic transport and structure evolution (the activation energy for bulk diffusion likely exceeds the value of 0.5 eV, the approximate upper limit for processes to be active at room temperature). Other complications are the behavior of the solid–electrolyte interface [31], which undergoes continuous evolution during battery operation, and the binder [32].

The existing methodologies for kinetic modeling include first principles theory [29,30] and molecular dynamics [33], which are restricted primarily to microscopic length and time scales, Monte Carlo lattice gas models [34], which extend to mesoscopic length and time scales and continuum and rate-theory models [35,36], which extend to macroscopic length and time scales. Continuum and rate-theory models are widely practiced in kinetic modeling. For example, they are commonly used to model diffusion limited growth of precipitates [37]. Electrochemical applications, compared with precipitate growth kinetics, have several additional complications, including external current, rupture and spallation, simultaneous diffusion of different components, diffusion governed by short circuit paths (planar and linear defects), the SEI, etc. These complications have thus far discouraged attempts to model intermetallic compound battery electrode kinetics.

11. Conclusions

We have argued earlier that the complexity of the materials processes and transformations that occur during battery operation make performance simulations for intermetallic compound electrodes intractable at this time. Nevertheless, in spite of our inability to model the overall kinetic behavior of the electrode, some thermodynamic and microscopic aspects of intermetallic electrodes can be modeled with reasonable reliability. These properties include the reaction voltage, discussed earlier, which first principles calculations typically overestimate slightly, but give the correct order of magnitude for. Such energy calculations, in conjunction with in situ structure measurements such as X-ray diffraction, can also help identify the actual sequence of reactions of Li with an intermetallic compound that occur during the insertion cycle. Another property that is accessible to theory is the partial molar volume for Li insertion into a metal. Theory can predict properties of intercalated (interstitial) lithium, such as site preference, solubility and perhaps activation energy for diffusion, although such calculations were not presented here. Therefore, although the overall reaction kinetics are beyond our present ability to model, theoretical predictions can be helpful in the interpretation of experiments on particular intermetallic compounds.

Acknowledgements

This work was supported at Argonne National Laboratory by the Chemical Sciences Division of the Office of Basic Energy Sciences of the US Department of Energy, under contract no. W31-109-Eng-38. Most of the computational work was performed at the National Energy Research Supercomputer Center.

References

[1] M.M. Thackeray, J.T. Vaughey, A.J. Kahaian, K.D. Kepler, R. Benedek, Intermetallic insertion electrodes derived from NiAs, Ni_2In, and Li_2CuSn-type structures for lithium-ion batteries, Electrochem. Commun. 1 (1999) 111–115.

[2] J.T. Vaughey, J. O'Hara, M.M. Thackeray, Intermetallic insertion electrodes with a zinc-blende-type structure for Li batteries: a study of Li_xInSb ($0 < x < 3$), Electrochem. Solid State Lett. 3 (2000) 13–16.

[3] L.M.L. Fransson, J.T. Vaughey, R. Benedek, K. Edstrom, J.O. Thomas, M.M. Thackeray, Phase transitions in lithiated Cu_2Sb anodes for lithium batteries: an in situ X-ray diffraction study, Electrochem. Commun. 3 (2001) 317–323.

[4] P. Villars, L.D. Calvert, Pearson's Handbook of Crystallographic Data for Intermetallic Phases, 2nd Edition, ASM, Materials Park, OH, 1991.

[5] X.B. Zhao, G.S. Cao, A study of Zn_4Sb_3 as a negative electrode of secondary lithium cells, Electrochim. Acta 46 (2001) 891–896.

[6] M. Winter, J.O. Besenhard, Electrochemical lithiation of tin and tin-based intermetallics and composites, Electrochim. Acta 45 (1999) 31–50.

[7] H. Li, L.H. Shi, W. Lu, X.J. Huang, L.Q. Shen, Studies on capacity loss and capacity fading of nanosized SnSb alloy anode for Li-ion batteries, J. Electrochem. Soc. 148 (1999) A915–A922.

[8] D. Larcher, L.Y. Beaulieu, O. Mao, A.E. George, J.R. Dahn, Study of the reaction of lithium with isostructural A_2B and various Al_xB alloys, J. Electrochem. Soc. 147 (2000) 1703–1708.

[9] F.J. Fernandez-Madrigal, P. Lavela, C. Perez-Vicente, J.L. Tirado, Electrochemical reactions of polycrystalline $CrSb_2$ in lithium batteries, J. Electroanal. Chem. 501 (2001) 205–209.
[10] J.T. Vaughey, et al., Unpublished work, 2000.
[11] R. Alcantara, F.J. Fernandez-Madrigal, P. Lavela, J.L. Tirado, J.C. Jumas, J.C. Olivier-Fourcade, Electrochemical reaction of lithium with the $CoSb_3$ skutterudite, J. Mater. Chem. 9 (1999) 2517–2521.
[12] X.B. Zhao, G.S. Cao, C.P. Lv, L.J. Zhang, S.H. Hu, T.J. Zhu, B.C. Zhou, Electrochemical properties of some Sb or Te based alloys for candidate anode materials of lithium-ion batteries, J. Alloys Compounds 315 (2001) 265–269.
[13] L.Y. Beaulieu, J.R. Dahn, The reaction of lithium with Sn–Mn–C intermetallics prepared by mechanical alloying, J. Electrochem. Soc. 147 (2000) 3237–3241.
[14] L.Y. Beaulieu, D. Larcher, R.A. Dunlap, J.R. Dahn, Reaction of lithium with grain-boundary atoms in nanostructured compounds, J. Electrochem. Soc. 147 (2000) 3206–3212.
[15] O. Mao, J.R. Dahn, Mechanically alloyed Sn–Fe(–C) powders as anode materials for Li-ion batteries. Part II. The SnFe system, J. Electrochem. Soc. 146 (2000) 414–422.
[16] O. Mao, R.L. Turner, I.A. Courtney, B.D. Fredericksen, M.I. Buckett, L.J. Krause, J.R. Dahn, Active/inactive nanocomposites as anodes for Li-ion batteries, Electrochem. Solid State Lett. 2 (1999) 3–5.
[17] G.M. Ehrlich, C. Durand, X. Chen, T.A. Hugener, F. Spiess, S.L. Suib, Metallic negative electrode materials for rechargeable nonaqueous batteries, J. Electrochem. Soc. 147 (2000) 886–891.
[18] D. Larcher, L.Y. Beaulieu, D.D. MacNeil, J.R. Dahn, In situ X-ray study of the electrochemical reaction of Li with eta'-Cu_6Sn_5, J. Electrochem. Soc. 147 (2000) 1658–1662.
[19] Y. Xia, T. Sakai, T. Fujieda, M. Wada, H. Yoshinaga, Flake CuSn alloys as negative electrode materials for rechargeable lithium batteries, J. Electrochem. Soc. 148 (2001) A471–A481.
[20] L. Fang, B.V.R. Chowdari, Sn–Ca amorphous alloy as anode for lithium ion battery, J. Power Sources 97/98 (2001) 181–184.
[21] W.J. Weydanz, M. Wohlfahrt-Mehrens, R.A. Huggins, A room temperature study of the binary lithium–silicon and the ternary lithium–chromium–silicon system for use in rechargeable lithium batteries, J. Power Sources 81/82 (1999) 237–242.
[22] G.X. Wang, L. Sun, D.H. Bradhurst, S. Zhong, S.X. Dou, H.K. Liu, Nanocrystalline NiSi alloy as an anode material for lithium-ion batteries, J. Alloys Compounds 306 (2000) 249–252.
[23] G.X. Wang, L. Sun, D.H. Bradhurst, S. Zhong, S.X. Dou, H.K. Liu, Innovative nanosize lithium storage alloys with silica as active center, J. Power Sources 88 (2000) 278–281.
[24] H. Kim, J. Choi, H.J. Sohn, T. Kang, The insertion mechanism of lithium into Mg_2Si anode material for Li-ion batteries, J. Electrochem. Soc. 146 (2001) 4401–4405.
[25] E. Cairns, presentation at this workshop.
[26] H. Schmalzried, Chemical Kinetics of Solids, VCH, Weinheim, 1995.
[27] R.A. Rapp, A. Ezis, G.J. Yurek, Displacement reactions in the solid state, Met. Trans. 4 (1973) 1283–1292;
G.J. Yurek, R.A. Rapp, J.P. Hirth, Kinetics of the displacement reaction between iron and Cu_2O, Met. Trans. 4 (1973) 1293–1300.
[28] R.A. Huggins, Lithium alloy negative electrodes, J. Power Sources 81/82 (1999) 13–19, discusses monatomic metal electrodes.
[29] G. Kresse, J. Furthmuller, Efficiency of ab initio total energy calculations for metals and semiconductors using a plane-wave basis set, Comput. Mater. Sci. 6 (1996) 15.
[30] G. Kresse, J. Furthmuller, Efficient iterative schemes for ab initio total energy calculations using a plane-wave basis set, Phys. Rev. B 54 (1996) 11169–11186.
[31] B.V. Ratnakumar, M.C. Smart, S. Surampudi, Effects of SEI on the kinetics of lithium intercalation, J. Power Sources 54 (2001) 137–139.
[32] M. Wachtler, M.R. Wagner, M. Schmied, M. Winter, J.O. Besenhard, The effect of the binder morphology on the cycling stability of Li-alloy composite electrodes, J. Electroanal. Chem. 510 (2001) 12–19.
[33] B. Ammundsen, J. Roziere, M.S. Islam, Atomistic simulation studies of lithium and proton insertion in spinel lithium manganates, J. Phys. Chem. B 101 (1997) 8156–8163.
[34] C. Wolverton, V. Ozolins, Entropically favored ordering: the metallurgy of Al_2Cu revisited, Phys. Rev. Lett. 86 (2001) 5518–5521.
[35] L. Song, J.W. Evans, Electrochemical-thermal model of lithium polymer batteries, J. Electrochem. Soc. 147 (2000) 2086–2095, and references therein.
[36] B. Kaplan, H. Groult, N. Kunagai, S. Komaba, F. Lantelme, Theoretical approach of the lithium intercalation/deintercalation process in host materials, Electrochemistry 69 (2001) 592–597.
[37] J.-Y. Huh, T.Y. Tan, U. Goesele, Model of partitioning of point defect species during precipitation of a misfitting compound in Czochralski silicon, J. Appl. Phys. 77 (1995) 5563–5571.